e-ISSN 2581-0405
Asian Journal of Applied Research for Community Development and Empowerment
Journal home page: http://ajarcde-safe-network.org ISSN 2581-0405

Integrated Analysis of Inverter Temperature Effects, Protection, and Zero-Export Control in On-Grid PV Systems

Achmad Zidan Alamsyah[1], Muhamad Iqbal Risantia[2], Wahyu Deka Setiyawan[3], Nur Alif Mardiyah[4], and Ilham Pakaya[5].*

[12345] *Department of Electrical Engineering, Faculty of Engineering, Universitas Muhammadiyah Malang, Malang. Indonesia*

ARTICLE INFO

Article History:
Received: 28 April 2026
Final Revision: 15 May 2026
Accepted: 16 May 2026
Online Publication: 18 May 2026

KEYWORDS

contribution, subsidized fertilizer, rice production, agricultural policies

CORRESPONDING AUTHOR

*E-mail: nuralif@umm.ac.id

A B S T R A C T

This study presents an integrated field-based assessment of inverter-room temperature effects, protection-system readiness, and zero-export control in a 33.04 kWp grid-connected photovoltaic (PV) system at an industrial facility in Indonesia. The study addresses a practical reliability gap by combining thermal analysis, before-interconnection protection review, and power-flow regulation in one framework. Field observations were conducted for two operating days from 10:00 to 15:00 at 15-minute intervals. The thermal assessment used 12 paired A/C ON and A/C OFF intervals with irradiance differences of 2-10 W/m² to minimize irradiance-related bias. A paired t-test, correlation analysis, and linear regression were applied. Increasing inverter-room temperature from 21.66 °C to 28.73 °C reduced average inverter output from 24.156 kW to 23.621 kW. The average reduction was 0.535 kW or 2.21%, with empirical sensitivity of 0.076 kW/°C and a statistically significant paired-output difference ($p < 0.001$). The protection assessment confirmed that the before-interconnection panel supports overcurrent interruption, surge mitigation, grounding, and local isolation, although detailed fault-current coordination and grounding-resistance tests were outside the present scope. Zero-export control reduced surplus grid export from 66.18 kWh to 0.00 kWh; the potential curtailed-energy share was 38.56%. These findings demonstrate that thermal control, protection readiness, and export regulation are complementary measures for improving industrial on-grid PV reliability in tropical operating conditions..

Contribution to Sustainable Development Goals (SDGs):
SDG 7: Affordable and Clean Energy
SDG 9: Industry, Innovation and Infrastructure
SDG 11: Sustainable Cities and Communities
SDG 13: Climate Action

1. INTRODUCTION

1.1. Research Background

Grid-connected photovoltaic (PV) systems are increasingly implemented in commercial and industrial facilities to reduce dependence on conventional grid electricity and support the renewable-energy transition. In practical installations, however, system performance is not determined only by installed PV capacity. Reliability also depends on the inverter operating environment, protection readiness before interconnection, and power-flow control when PV production differs from the actual load.

The inverter is the main component that changes DC power from PV modules into AC power synchronized with the utility grid. The observed system used a 33.04 kWp PV array consisting of Jinko photovoltaic modules [4] and one Huawei SUN2000-

This work is licensed under a Creative Commons Attribution-NonCommercial-ShareAlike 4.0 International License
Published under licence by SAFE-Network

30KTL-M3 inverter. The inverter is specified with high conversion efficiency and built-in protection features, but it still operates within thermal limits. The manual states that the M3 series operates at ambient temperatures from -25 °C to +60 °C, with derating above +45 °C [3]. Thus, thermal condition remains a practical reliability factor even when the inverter has high rated efficiency.

In tropical industrial buildings, inverter rooms may accumulate heat because of roof exposure, limited natural ventilation, enclosure geometry, and equipment placement. These conditions can increase local room temperature around the inverter and may influence output stability, component stress, and long-term reliability. Therefore, a field-based assessment is needed to examine whether inverter-room temperature control contributes to more stable PV operation under actual industrial conditions.

1.2. Literature Review

Previous research on a grid-connected inverter installed in Thailand reported that high ambient temperature negatively affects PV system performance and that maximum inverter efficiency dropped by up to 2.5% when ambient temperature exceeded 37 °C [1]. Recent PV reliability studies also emphasize that inverter thermal characteristics influence long-term reliability and that high-temperature stress is relevant to inverter degradation [13], [14]. Thermal and inverter monitoring data have also been used to support PV fault detection and reliability assessment [9].

PV integration into local distribution networks can affect power-flow behavior when generation and load are not balanced [8], [10]. For on-grid PV systems, protection before interconnection is also necessary because the PV system is connected to facility distribution panels and the utility network. Overcurrent, surge, short-circuit, and grounding protection are required to reduce equipment and safety risks. Interconnection standards and application guides emphasize technical performance, operation, safety, and maintenance requirements for distributed energy resources [5], [6], while IEC 60364-7-712 provides requirements for low-voltage PV power-supply installations [7].

In Indonesia, power-flow management is increasingly important because surplus energy exported to the grid of the Electricity Supply Business License holder is not calculated in customer billing [2]. Recent zero-export research also identifies reverse power flow and export restriction as practical drivers for feed-in prevention in grid-connected PV systems [15]. These previous studies and standards show the importance of thermal behavior, protection readiness, and export limitation; however, these aspects are commonly discussed separately rather than as one integrated operational reliability framework.

1.3. Research Objective

Unlike previous studies that separately investigate inverter thermal behavior, protection systems, or export limitation, this study integrates these three operational reliability dimensions into a unified field-based assessment framework for an industrial PV system operating in a tropical environment. This integration is scientifically important because thermal instability, protection readiness, and export control affect the same operational objective: maintaining reliable, safe, and regulation-compliant PV operation.

The methodological gap addressed by this work is the lack of applied field assessments that combine paired thermal comparison, protection-readiness mapping, and zero-export energy-flow evaluation in one industrial PV case study. Therefore, this study evaluates a 33.04 kWp on-grid PV system by integrating inverter-room thermal analysis, before-interconnection protection assessment, and zero-export control evaluation. The objective is to provide an applied reliability assessment that is technically useful for industrial PV operators and aligned with sustainable energy implementation.

2. MATERIALS AND METHODS

2.1. Research object and system specification

The research object was a 33.04 kWp on-grid PV system located at PT Faber-Castell International Indonesia. The system used 56 Jinko JKM585-72HL4-(V) modules and one Huawei SUN2000-30KTL-M3 three-phase grid-connected inverter. The inverter was installed in an upper-floor room with limited natural ventilation; therefore, an air-conditioning unit was used as the thermal-control variable.

Table 1. Main specification of the observed system.

Parameter	Description
Installed PV capacity	33.04 kWp
PV module	Jinko JKM585-72HL4-(V), 56 units
Inverter	Huawei SUN2000-30KTL-M3
Grid output	380 V AC, 50 Hz
Thermal variable	A/C ON and A/C OFF
Protection focus	MCCB, SPD, fuse, grounding
Power-flow control	DTSU666-H meter, CT sensors, inverter communication

2.2. Field data collection and paired-comparison criteria

Field data were recorded over two operating days at 15-minute intervals from 10:00 to 15:00. The variables included time, A/C condition, load, inverter-room temperature, inverter output, ambient-temperature range, and irradiance. The two days were used as a preliminary field assessment because it captured normal daytime operation, repeated A/C ON/OFF conditions, and the irradiance range in which the inverter produced stable mid-day output. The results are therefore interpreted as site-specific preliminary evidence rather than a universal long-term thermal model.

The paired-comparison method was used to minimize irradiance-related bias in inverter-output analysis. Six paired intervals were selected from each observation day, covering 10:30-13:15. Pair matching was accepted when the absolute irradiance difference between A/C ON and A/C OFF intervals was no greater than 10 W/m². Across 12 paired intervals, the irradiance difference ranged from 2 to 10 W/m², with an average of 6.25 W/m², approximately 0.69% of the paired average irradiance.

https://doi.org/10.29165/ajarcde.v10i2.1048

Table 2. Pair-matching transparency used for thermal comparison.

Criterion	Value
Window	10:00–15:00, 15-min interval, 2 days
Subset	12 pairs from 10:30–13:15
Pairs	6 pairs Day 1; 6 pairs Day 2
Basis	A/C ON vs A/C OFF at comparable irradiance
Tolerance	Max $\|\Delta G\|$ = 10 W/m²
Actual ΔG	2–10 W/m²; mean 6.25 W/m² (~0.69%)
Variables	T_room, P_out, irradiance, load, A/C status
Purpose	Reduce irradiance-related bias before output comparison
Data note	Processed pair-level data available upon academic request, subject to site permission

The percentage reduction in inverter output was calculated using Eq. (1).

$$\text{Power reduction (\%)} = [(P_ON - P_OFF) / P_ON] \times 100 \quad (1)$$

2.3. *Statistical analysis*

Mean, standard deviation, and 95% confidence interval were calculated for the paired output difference. A paired t-test was used to examine whether the inverter output under A/C ON differed from the output under A/C OFF. Pearson correlation and simple linear regression were used to describe the temperature-output relationship. Because irradiance remains the dominant physical input to PV generation and because the observation was limited to two operating days, the regression result was interpreted as descriptive supporting evidence rather than a standalone causal model.

2.4. *Protection and zero-export assessment*

The protection subsystem was evaluated based on the panel design before interconnection, system documentation, and ETAP simulations, in accordance with the principles of IEE 157 and IEC 60364-7-712. The evaluation covered overcurrent protection, transient overvoltage mitigation, local isolation, and system maintainability [5], [7]. The protection system uses an iPF40 3p+N SPD on the AC side to protect the system from transient surges caused by lightning or distribution network switching. Protection analysis was performed using Time Current Characteristic (TCC) and arc flash simulations to evaluate protection coordination, MCCB selectivity, fault current, protection operating time, and fault energy at the interconnection point. This research is still limited to simulation validation; therefore, grounding resistance measurements, experimental verification of SPD performance, and direct protection testing in the field have not yet been conducted.

The zero-export subsystem was assessed by comparing energy-flow scenarios before and after control activation. The installed zero-export function used an energy meter and current transformers as feedback elements for inverter power limitation. The assessment focused on accumulated import/export energy because detailed transient response time, protocol-level communication logs, and packet-level delay were not available from the monitoring record. Potential curtailed energy was calculated using Eq. (2).

$$E_curtailed = E_PV - E_load \quad (2)$$

3. RESULT AND DISCUSSION

3.1. *Thermal response and paired output comparison*

The A/C ON condition maintained the inverter-room temperature within approximately 21.5-22.4 °C. When the A/C was OFF, the temperature increased to approximately 26.0-31.1 °C. The absolute inverter output was still strongly influenced by irradiance; however, under paired intervals with comparable irradiance, output during A/C OFF was generally lower than output during A/C ON.

Table 3. Summary of paired thermal comparison.

Parameter	Result
Day 1 average output	A/C ON 24.395 kW; A/C OFF 23.918 kW; reduction 1.96%
Day 2 average output	A/C ON 23.918 kW; A/C OFF 23.324 kW; reduction 2.48%
Combined average temperature	A/C ON 21.66 °C; A/C OFF 28.73 °C; increase 7.07 °C
Combined average irradiance	A/C ON 899.92 W/m²; A/C OFF 899.33 W/m²; relatively comparable
Combined average output	A/C ON 24.156 kW; A/C OFF 23.621 kW; reduction 0.535 kW (2.21%)

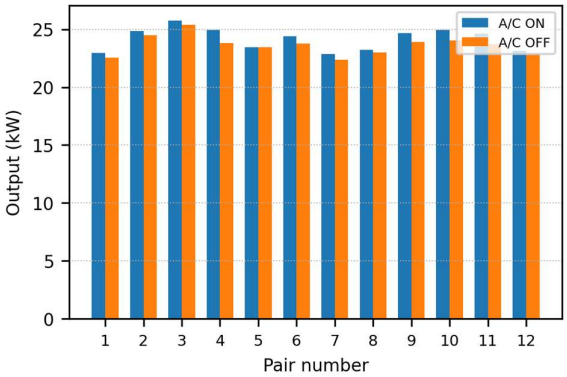

Fig. 2. Inverter output under 12 paired comparable-irradiance intervals. Pair numbers 1–6 represent Day 1 and 7–12 represent Day 2. Data source: field measurements and processed paired dataset.

The combined paired data show that inverter-room temperature increased from 21.66 °C to 28.73 °C, while average irradiance remained comparable at 899.92 W/m² and 899.33 W/m². Average inverter output decreased from 24.156 kW to 23.621 kW. The reduction was 0.535 kW or 2.21%, with empirical sensitivity of approximately 0.076 kW/°C.

3.2. *Statistical and regression analysis of thermal effect*

Table 4. Statistical summary of the paired thermal analysis.

Parameter	Value
Number of paired intervals	12

Irradiance difference tolerance	2-10 W/m²; mean 6.25 W/m²
A/C ON output	24.156 ± 0.961 kW
A/C OFF output	23.621 ± 0.849 kW
Mean output reduction	0.535 ± 0.328 kW
95% confidence interval	0.327 to 0.744 kW
Paired t-test	t(11) = 5.651; p = 0.00015
Pearson correlation	r = -0.262; p = 0.216
Regression equation	P_out = 25.530 - 0.065T_room
R^2	0.069

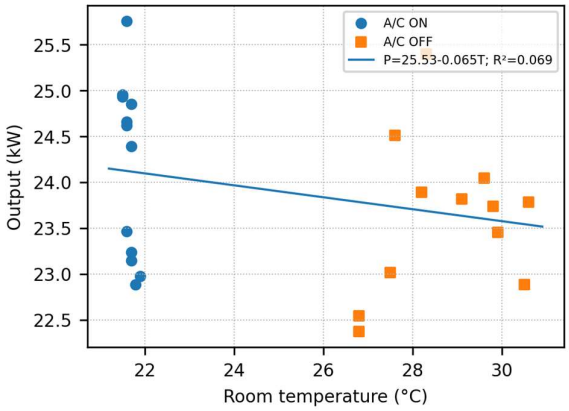

Fig. 3. Scatter plot and simple regression between inverter-room temperature and inverter output power using paired observation data. Axis units are °C and kW. Data source: processed field measurements.

The paired t-test indicates that the output difference between A/C ON and A/C OFF conditions was statistically significant at the 95% confidence level. The 95% confidence interval of the mean output reduction ranged from 0.327 to 0.744 kW, indicating that the reduction was consistently positive across the paired dataset. The simple temperature-output regression produced a negative slope, but the coefficient of determination was low (R^2 = 0.069). This is physically reasonable because PV output is controlled not only by inverter-room temperature but also by irradiance, MPPT operation, load condition, and time-varying system behavior. Therefore, the regression is interpreted as descriptive evidence, while paired comparison provides the main thermal interpretation.

3.3. Protection-system readiness and verification scope

The before-interconnection panel improves reliability by providing a structured point between inverter output and facility distribution. The panel integrates protection and isolation functions so that disturbances can be localized and maintenance activities can be conducted more safely.

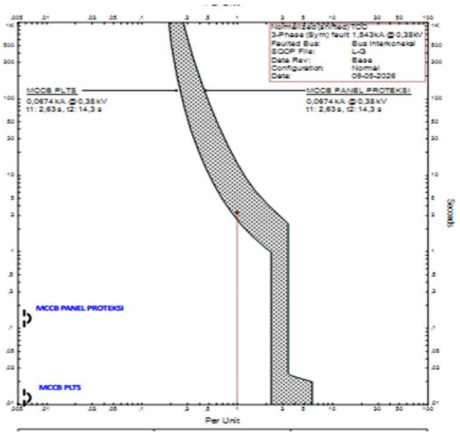

Fig. 4 Result of Time-Current Characteristic Curve Visualization Protection coordination analysis was performed using Time Current Characteristic (TCC) simulations in ETAP to evaluate the selectivity of the MCCB during a fault. The simulation result show that the protection panel MCCB trips before the PV system MCCB when a fault occurs on the interconnection bus with a fault current of 1.543 kA at a voltage of 0.38 kV and a trip time of approximately 2.63 seconds. These conditions indicate that the protection coordination, whereby the protection device closest to the fault point will trip first to isolate the fault before it reaches the inverter of the main system. Thus, the use of a protection panel before the interconnection is capable of improving the safety, reliability, and operational continuity of the on-grid PV system.

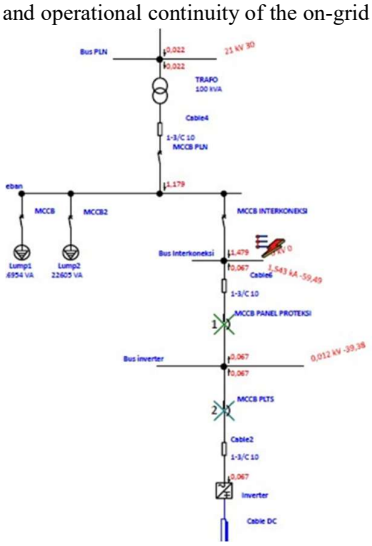

Fig. 5. Single Line Diagram

An arc flash simulation was conducted to determine the level of fault energy and safety risks at the system interconnection point. The simulation results show that the arc flash energy at the interconnection busbar is 54.3 cal/cm^2 with a protection boundary of approximately 59.49 cm. This value indicates that the interconnection point is the area with the highest fault risk because it is the meeting point between the PV inverter, the utility grid, and the load. Nevertheless, the presence of a protection panel before the interconnection helps limit the impact of fault energy through the operation of the MCCB, which selectively interrupts the fault current. These simulation results demonstrate that the protection system not only enhances system reliability but also supports operational safety in accordance with the principles of electrical power system protection.

https://doi.org/10.29165/ajarcde.v10i2.1048

Table 5. Protection-readiness mapping and verification scope.

Aspect	Finding
Overcurrent protection	MCCB is available; ETAP simulations indicate a fault current of 1,543 kA
Surge mitigation	iPF40 3P+N SPD is installed on the AC side; experimental surge performance testing has not yet been conducted
Grounding paths	Grounding is available at the protection panel; grounding resistance has not yet been measured directly
Fault isolation	TCC curve simulations show that the protection panel's MCCB trips first to isolate the fault
Maintenance readiness	Protection components are grouped and easily accessible, facilitating maintenance and local system isolation

The observed panel configuration is consistent with functional requirements for a safer PV interconnection point because it provides overcurrent protection, surge mitigation, grounding connection, and local isolation. Nevertheless, future work should include fault-current calculation, time-current coordination, SPD specification verification, and grounding-resistance measurement to confirm protection performance quantitatively.

3.4. Zero-export power-flow control and curtailed-energy estimation

The zero-export assessment showed that the control system prevented surplus PV energy from flowing to the utility grid when PV production exceeded load demand. Before zero-export activation, the PV-greater-than-load scenario recorded 66.18 kWh of exported energy. After zero-export activation, grid export became 0.00 kWh because the inverter output was limited according to internal load demand.

Table 6. Energy-flow and curtailed-energy assessment.

Scenario	Result
Before control, load > PV	PV 111.32 kWh; load 328.64 kWh; import 217.32 kWh; export 0.00 kWh
Before control, PV > load	PV 171.63 kWh; load 105.45 kWh; export 66.18 kWh
After control, PV = load	PV 109.21 kWh; load 109.21 kWh; import/export 0.00 kWh
After control, load > PV	PV 171.57 kWh; load 341.20 kWh; import 169.63 kWh; export 0.00 kWh
Potential curtailed/surplus energy	66.18 kWh, equal to 38.56% of PV production in PV > load case

Fig. 6. DTSU666-H smart power sensor and Current Transformer (CT) used in the zero export

The zero-export system operates by utilizing the DTSU666-H Current Transformer (CT), which is installed at the Point of Common Coupling (PCC) to continuously monitor the direction of current, voltage, and power flow between the PV system, the load, and the PLN grid. The components of the zero-export system used are shown in Figure 4. Measurement data from the DTSU666-H is transmitted to the Huawei inverter via RS485 communication using the Modbus RTU protocol, enabling the inverter to perform real-time power control with rapid response to changes in load and PV system energy production, thereby reducing energy export to the PLN grid to near zero. Based on load demand data, the inverter automatically adjusts its output power to prevent reverse power flow into the PLN grid. During the monitoring process, no significant export overshoot was observed under varying load conditions, indicating that the control system effectively responds to power changes.

The implementation of the zero-export system successfully reduced energy exported to the PLN grid to nearly 0.00 kWh. However, the inverter's power limitation prevents some of the potential energy from the PV system from being utilized when energy production exceeds load demand. This condition is referred to as curtailment loss. The amount of unused energy can be calculated using the equation:

$$E_{curtailed} = E_{PV} - E_{load}$$

Based on the monitoring data in Table 4, the solar power plant generated 171.63 kWh of energy, while the load consumption was 105.45 kWh, resulting in an energy curtailment of 66.18 kWh. The curtailment percentage is calculated as follows:

$$Curtailment\ (\%) = \frac{66.18}{171.63} \times 100 = 38.56\%$$

The results show that the zero-export system is effective in preventing energy from being exported to the PLN grid, even though some of the solar energy cannot be fully utilized due to the inverter's output power limitations.

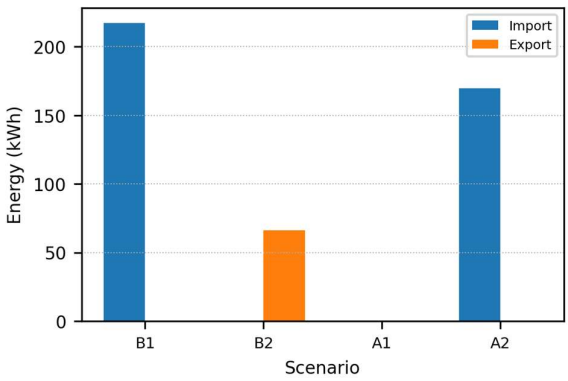

Fig. 7. Grid import/export before and after zero-export control. B1 and B2 are before-control scenarios; A1 and A2 are after-control scenarios. Axis units are kWh. Data source: monitored energy-flow records.

The curtailed or surplus-energy indicator was 66.18 kWh, equal to 38.56% of PV production in the PV-greater-than-load scenario. Operationally, this value represents energy that must be consumed by internal loads, shifted to another load period, stored in a battery-energy storage system, or limited by the inverter under zero-export operation. Zero-export control does not increase PV generation; it improves regulatory and operational suitability by preventing non-beneficial reverse power flow.

The present data record did not include high-speed transient logs; therefore, zero-export response time and short-duration export overshoot could not be quantified. The available monitoring data indicate that accumulated grid export became 0.00 kWh after the control function was active. Future studies should log second-level meter data to evaluate transient overshoot, communication delay, and dynamic inverter response.

3.5. Critical discussion: thermal sensitivity, tropical condition, and operating trade-off

The empirical sensitivity of 0.076 kW/°C was lower than the efficiency deterioration reported in studies where ambient temperature exceeded 37 °C [1]. This difference is expected because the inverter-room temperature in the present observation mostly remained below 32 °C, which is below the derating temperature stated in the inverter specification [3]. The observed reduction therefore reflects operational stability under moderate thermal stress, not a maximum-temperature failure scenario.

Tropical industrial environments may create unique thermal conditions because roof exposure, limited ventilation, closed electrical rooms, and heat emitted by surrounding equipment can raise local inverter-room temperature even when outdoor ambient range appears acceptable. The upper-floor placement of the inverter can also increase heat accumulation because warm air tends to collect in upper building zones.

The practical value of A/C use should be interpreted carefully. Cooling the inverter room can help stabilize output and reduce thermal stress, but the air-conditioning unit also consumes energy. Therefore, the recommended strategy is operational thermal management rather than uncontrolled cooling: maintaining ventilation, avoiding direct heat accumulation, checking A/C condition during high-irradiance periods, and monitoring inverter temperature trends. Passive ventilation improvement, room insulation, or inverter relocation may be evaluated before increasing active cooling capacity.

The integrated reliability perspective is important because thermal control, protection readiness, and zero-export regulation affect different loss mechanisms. Thermal control reduces output instability and component stress. Protection readiness reduces risk propagation during electrical disturbances. Zero-export control prevents non-beneficial energy export and improves compliance with the current Indonesian rooftop-PV billing context.

3.6. Integrated reliability implication and SDG relevance

Reliable PV operation supports SDG 7 by improving renewable-energy utilization, SDG 9 by strengthening industrial energy infrastructure, SDG 11 by encouraging cleaner urban-industrial facilities, and SDG 13 by supporting lower-carbon electricity use. These contributions are practical because they are based on an existing operating PV system and directly address maintenance, safety, and energy-use challenges.

3.7. Limitations and future work

The main limitation of this study is that the field observation covered only two operating days. Therefore, the thermal coefficient, statistical results, and temperature-output relationship should be interpreted as preliminary and site-specific findings rather than as a universal long-term thermal-performance model. The observed days represented normal daytime operation at the investigated facility, including repeated A/C ON and A/C OFF conditions and stable mid-day irradiance ranges. However, the short observation period did not capture broader environmental variability.

Weather conditions may vary from day to day and even within the same day due to cloud movement, rainfall potential, wind conditions, humidity changes, and ambient-temperature fluctuations. These factors can directly affect solar irradiance, inverter-room temperature, and inverter output power. In addition, seasonal differences between dry and rainy periods in tropical regions may produce different irradiance stability, thermal accumulation patterns, and cooling requirements. Long-term irradiance fluctuations, dust accumulation, and changes in building heat gain were also not included in the present observation. For this reason, the results should be considered as field-based preliminary evidence for the investigated industrial PV system, not as a general model for all on-grid PV systems.

Another limitation is that the study used inverter-room temperature rather than direct internal inverter temperature. Although room temperature is relevant for evaluating the thermal condition around the inverter, internal inverter temperature would provide a more direct indication of component-level thermal stress. Future research should integrate inverter internal-temperature data from the monitoring platform to improve the accuracy of thermal-performance evaluation.

The assessment of the protection system in this study is still limited to an evaluation of design readiness, ETAP simulation results, and functional observations of the system. Although protection coordination simulations using TCC curves and arc flash simulations have been conducted to evaluate the MCCB response during a fault, this study has not yet included detailed fault current calculations, experimental verification of SPD performance and types, or direct on-site measurements of grounding resistance. Therefore, the validation of the protection

https://doi.org/10.29165/ajarcde.v10i2.1048

system in this study is still limited to a simulation approach and does not fully represent the actual operational conditions of an on-grid PV system.

The zero-export assessment was based on accumulated energy-flow data before and after control activation. High-speed transient measurements were not available; therefore, zero-export response time, communication delay, and short-duration export overshoot could not be quantified. Future research should use second-level or sub-second monitoring data to evaluate transient export behavior, meter-inverter response time, and dynamic inverter power-limiting performance.

Future work should extend the observation period to several weeks or months, include different weather and seasonal conditions, measure humidity and ventilation rate, record inverter internal temperature, and evaluate the economic trade-off between cooling-energy consumption, inverter-output stability, and zero-export curtailment. Further analysis of battery-energy storage or load-shifting strategies may also be conducted to improve PV self-consumption when surplus energy frequently occurs.

3.8. Operational recommendations for similar industrial PV systems

Table 7. Recommended actions for improving on-grid PV reliability.

Issue	Recommended action
High inverter-room temperature	Maintain ventilation or room cooling and inspect A/C performance periodically
Unclear fault-isolation point	Use a before-interconnection panel with clear labeling and accessible switching
Surge and transient risk	Install and routinely inspect SPD condition indicators
Uncontrolled surplus export	Activate zero-export control and verify meter-CT orientation
Short-term data uncertainty	Use longer monitoring periods and compare data at similar irradiance
Energy curtailment	Consider load shifting or future battery storage when surplus is frequent

The most practical first step is not to overspecify new equipment but to improve operational discipline. The inverter room should be inspected during high-irradiance and high-ambient-temperature periods. Protection components should be checked for physical condition, labeling, and tightening. The zero-export setting should be validated after commissioning because CT polarity or communication errors may cause inaccurate export limitation.

4. CONCLUSION

This study assessed the reliability of a 33.04 kWp on-grid PV system by integrating inverter-room thermal management, before-interconnection protection assessment, and zero-export control. The novelty lies in the unified field-based assessment of three operational reliability dimensions that are often examined separately. The paired observation showed that increasing inverter-room temperature from 21.66 °C to 28.73 °C reduced average inverter output from 24.156 kW to 23.621 kW under comparable irradiance. The reduction was 0.535 kW or 2.21%, with empirical sensitivity of 0.076 kW/°C. The paired t-test confirmed that the output difference was statistically significant ($t(11) = 5.651$; $p = 0.00015$), while regression analysis showed a negative but weak direct temperature-output relationship because irradiance and operating conditions also influenced output.

The pre-interconnection panel enhances system reliability and safety through overcurrent protection, surge mitigation using SPDs, grounding, isolation of local faults, and ease of maintenance. TCC simulation results show that the protection panel's MCCBs trip first during a fault, allowing the fault to be isolated before it reaches the inverter or the main system. Additionally, arc flash simulations demonstrate that the protection system helps reduce the impact of fault energy. However, comprehensive validation of the protection system still requires detailed fault current calculations, SPD verification, and direct on-site measurements of grounding resistance. The zero-export assessment showed that surplus grid export decreased from 66.18 kWh to 0.00 kWh after control activation when PV production exceeded load demand. The potential curtailed or surplus-energy share in that scenario was 38.56% of PV production. Overall, reliable industrial PV operation requires not only installed PV capacity but also controlled thermal conditions, protection readiness, and real-time power-flow regulation.

ACKNOWLEDGMENTS

The authors acknowledge PT Jayatama Adi Sentosa, PT Faber-Castell International Indonesia, and the site operator for supporting access to field observation and technical documentation. The authors also thank the Department of Electrical Engineering, Faculty of Engineering, Universitas Muhammadiyah Malang, for academic supervision and guidance.Generative AI disclosure: This manuscript utilized ChatGPT (OpenAI) for drafting text, article structuring, and grammar refinement. All research content, data interpretation, statistical results, and references were reviewed and validated by the authors.

REFERENCE

[1] K. Chumpolrat, V. Sangsuwan, N. Udomdachanut, S. Kittisontirak, S. Songtrai, P. Chinnavornrungsee, A. Limmanee, J. Sritharathikhun, and K. Sriprapha, "Effect of Ambient Temperature on Performance of Grid-Connected Inverter Installed in Thailand," International Journal of Photoenergy, vol. 2014, Article ID 502628, 2014, doi: 10.1155/2014/502628.

[2] Ministry of Energy and Mineral Resources of the Republic of Indonesia, "Regulation of the Minister of Energy and Mineral Resources Number 2 of 2024 concerning Rooftop Solar Power Plants Connected to the Electric Power Network of IUPTLU Holders," 2024.

[3] Huawei Technologies Co., Ltd., "SUN2000-(20KTL, 29.9KTL, 30KTL, 36KTL, 40KTL)-M3 Series User Manual: Technical Specifications," Huawei Enterprise Support, 2025.

[4] Jinko Solar Co., Ltd., "JinkoSolar Photovoltaic Modules Installation Manual," Jinko Solar, 2024.

[5] IEEE Standards Association, "IEEE Standard for Interconnection and Interoperability of Distributed Energy

Resources with Associated Electric Power Systems Interfaces," IEEE Std 1547-2018, 2018.

[6] IEEE Standards Association, "IEEE Application Guide for IEEE Std 1547-2018," IEEE Std 1547.2-2023, 2023.

[7] International Electrotechnical Commission, "IEC 60364-7-712: Low-voltage electrical installations - Part 7-712: Requirements for special installations or locations - Solar photovoltaic (PV) power supply systems," IEC, 2017.

[8] Q. Alsafasfeh, O. A. Saraereh, I. Khan, and S. Kim, "Solar PV Grid Power Flow Analysis," Sustainability, vol. 11, no. 6, 1744, 2019, doi: 10.3390/su11061744.

[9] O. Baltaci, Z. Kiral, K. Dalkilinc, and O. Karaman, "Thermal Image and Inverter Data Analysis for Fault Detection and Diagnosis of PV Systems," Applied Sciences, vol. 14, no. 9, 3671, 2024, doi: 10.3390/app14093671.

[10] M. H. Athari, Z. Wang, and S. H. Eylas, "Time-Series Analysis of Photovoltaic Distributed Generation Impacts on a Local Distributed Network," in 2017 IEEE Manchester PowerTech, Manchester, UK, 2017, pp. 1-6, doi: 10.1109/PTC.2017.7980908.

[11] S. Sugianto, "Comparative Analysis of Solar Cell Efficiency between Monocrystalline and Polycrystalline," INTEK: Jurnal Penelitian, vol. 7, no. 2, pp. 92-100, 2020.

[12] P. Hersch and K. Zweibel, Basic Photovoltaic Principles and Methods, Golden, CO: Solar Energy Research Institute, 1982.

[13] T. Li, S. Tao, R. Zhang, Z. Liu, L. Ma, J. Sun, and Y. Sun, "Reliability Evaluation of Photovoltaic System Considering Inverter Thermal Characteristics," Electronics, vol. 10, no. 15, 1763, 2021, doi: 10.3390/electronics10151763.

[14] M. Z. U. A. Afridi, S. Tatapudi, J. Flicker, D. Srinivasan, and G. Tamizhmani, "Reliability of Microinverters for Photovoltaic Systems: High-Temperature Accelerated Testing with Fixed and Cyclic Power Stresses," Energies, vol. 16, no. 18, 6511, 2023, doi: 10.3390/en16186511.

[15] J. Prasanth Ram, Y.-J. Kim, and D. Mathew, "A Grid-Safe and Efficiency-Optimized Architecture for Next-Generation Photovoltaic String Inverters under Feed-in Prevention and PV Export Conditions," Renewable Energy, vol. 263, 125433, 2026, doi: 10.1016/j.renene.2026.125433.

 https://doi.org/10.29165/ajarcde.v10i2.1048